Application of magnetite nanoparticles modified Azolla as an adsorbent for removal of reactive yellow dye from aqueous solutions

Fatemeh Shariati[a,*], Shahab Shariati[b], Mohammad Ali Amiri Moghaddam[b]

[a]Department of Environment, Lahijan Branch, Islamic Azad University, Lahijan, Iran, Tel. +989113334192/+981341230058,
Fax: +981341230058; email: shariati@liau.ac.ir
[b]Department of Chemistry, Rasht Branch, Islamic Azad University, Rasht, Iran, Tel. +989113314086;
email: Shariaty@iaurasht.ac.ir (Sh. Shariati), Tel. +989119338774; email: Mohammadali_amiri68@yahoo.com (M.A. Amiri Moghaddam)

ABSTRACT

In this study, we aimed to remove reactive yellow 160 (RY 160) dye from aqueous solutions, and for this, collected Azolla was modified with magnetite nanoparticles. The size and structure of magnetite modified Azolla nanocomposite were studied by scanning electron microscopy and Fourier-transform infrared spectroscopy. The factors affecting the dye removal efficiency including pH, ionic strength, stirring time, solution volume, and adsorbent weight were investigated using Taguchi fractional orthogonal array design (OA_{16}). The results of adsorption kinetics at 50 and 100 mg L^{-1} under optimum conditions (pH = 2, ionic strength = no salt addition, the solution volume = 25 mL, stirring time = 10 min and adsorbent weight = 0.15 g) showed that removal of RY 160 was performed through a pseudo-second-order kinetic model (q_e = 30.2 mg g^{-1}, R^2 = 1). Isotherm models at three contact times of 10, 25, and 50 min showed that adsorption follows the Freundlich model (n = 1.2, K_F = 2.3). Reusability experiments under optimum conditions confirmed the removal efficiency of more than 95% after 16 repetitive adsorption usage. The results of real samples showed that this nanocomposite is an effective adsorbent for the rapid removal of RY 160. Low-cost, reusability and fast elimination have made the synthesized nanocomposite as a useful adsorbent in RY 160 removal.

Keywords: Adsorption; Azolla; Magnetic nanoparticles; Magnetite; Reactive yellow 160

1. Introduction

Industrial wastewaters are the most important environmental pollutants and finding methods for reducing their hazards is a research priority. Dyes are chemical matters that are used in many industries including textiles, tannery, paper and pulp, plastic, and food. They are very considerable because of their toxicity for living organisms, disturbance in the performance of current treatment systems, and the interference in water ecology. For this reason, finding cheap and affordable methods for dyes removal from wastewaters has particular importance. Most dyes applied in the textile industry are non-biodegradable [1]. The most serious problem is from reactive and acidic dyes [2]. Reactive dyes are water–soluble and their removal with coagulation and biodegradation is very difficult. These dyes are chemically persistent and have very low biodegradability [3–5]. The adsorption on inexpensive adsorbents is a suitable and economical method for colored effluent decontamination [6–8]. Adsorption by nanoparticles is an environmentally friendly technology that is considered as an effective factor in the decontamination of polluted wastewater in recent years [3,8]. Magnetic nanoparticles due to easy separation with an external magnet attracted much attention [9,10].

* Corresponding author.

Iron nanoparticles especially superparamagnetic Fe_3O_4 nanoparticles (magnetite) have been more prominent due to abundance, cheapness, non-toxicity, good biocompatibility, lack of residual magnetism after external magnetic field removal, and high efficiency in the uptake of pollutants from contaminated waters [11–13].

Azolla is a fern with small leaves of dark green or reddish-brown with a length of 2.5 cm. This plant was first identified in 1873 and six species have been recorded worldwide. Azolla is the fern floating in the freshwater that has a symbiosis with the algae Anabaena. Azolla fern is one of the exotic plant species introduced to Iran and has dominated most of the marshes, wetlands, and paddy fields in the north of the country in recent decades. But there are also other countries such as Australia, New Zealand, England, Germany, etc. Suspended roots of Azolla absorb all or most of the water solids and spend them for growth and reproduction. Azolla entered Iran for nitrogen fixation and crop growth in paddy fields, but today it itself has become an environmental problem [14–18].

In this study, magnetite Azolla nanocomposites (MNCs) were synthesized in a very simple and easy process and were used to remove the reactive yellow 160 (RY 160) anionic dye for the first time. The idea of using Azolla as an adsorbent is due to its high adsorption capacity, low cost, and abundance in Anzali Wetland and other ponds of Iran. This application can help the environment because the aquatic ecosystem gets rid of the Azolla problem. For this purpose, the magnetite Azolla nanocomposite (Azolla@Fe_3O_4) was synthesized by the chemical co-precipitation method. Then, the effect of different variables on the adsorption process was investigated by Taguchi orthogonal array design method. Also, isotherm and kinetic models were evaluated to show the rate and capacity of the adsorption process. In this study, it was tried to use Azolla ferns as a natural and inexpensive adsorbent to remove RY 160 pollutants from the aquatic environment. This research could be a prelude to using this sorbent to remove all kinds of organic and color pollutants from the aquatic environment.

2. Materials and methods

2.1. Chemicals and instruments

All of the chemicals including iron(III) chloride hexahydrate ($FeCl_3·6H_2O$, 99.0%), iron(II) chloride tetrahydrate ($FeCl_2·4H_2O$, 99.7%), and ammonia (NH_4OH, 28% w/w) were supplied from Merck (Darmstadt, Germany). Azolla collected from Anzali Wetland, double distilled water, reactive yellow 160 dye ($C_{25}H_{22}ClN_9Na_2O_{12}S_3$, RY 160, Fig. 1), sieve with mesh 20 (equivalent to 0.0341-inch pore diameter), filter with 200 mesh (equivalent to 0.0029-inch pore diameter), Agate Mortar, 500 mL Pyrex three-necked flask, 6300 pc dual-beam UV-Vis spectrophotometer manufactured by MAPADA (China), pH Meter (EDT, model GP353, UK), magnetic stirrer (model L81, LABINCO, The Netherlands), digital weighing scale with precision 0.0001 g (model FA2004B, oven (Memmert, Germany), Fourier-transform infrared spectroscopy (FT-IR) instrument (Shimadzu 8900, Japan), and nitrogen gas (99%) for deoxygenating the solutions were used. In order to magnetic separation, a powerful super magnet (1 cm × 3 cm × 5 cm, 1.4 T) was used. The surface morphology and size of MNCs were determined by scanning electron microscopy (SEM) (Philips XL-30, The Netherlands). Energy-dispersive X-ray spectroscopy (EDX, model LEO1430VP, England, and Germany) was used to observe the elemental analysis.

2.2. Azolla powder preparation

Firstly, Azolla (*Azolla filiculoides* Lam) was collected from Anzali Wetland and paddy fields of Gilan Province. Then, it was washed twice with tap water and three times with double distilled water. For the preparation of Azolla powder, the purified Azolla was dried at 60°C and grounded in mortar. The resulting powder was sieved through a 200 mesh to produce a powder of fewer than 74 μm diameter. In order to modify the surface of these particles and create magnetic properties to facilitate their separation, magnetite nanoparticles were synthesized on the surface of Azolla powder by the chemical co-precipitation method.

2.3. Synthesis of magnetite Azolla nanocomposite (Azolla@Fe_3O_4 MNCs)

Magnetite Azolla nanocomposites were synthesized by the co-precipitation method from iron(III) and (II) chloride precursors at a molar ratio of 1:2. Magnetite nanoparticles were synthesized according to our previous studies [19–21]. First, a solution of 50 mL of iron salts (10.8 g $FeCl_3·6H_2O$, 4.0 g $FeCl_2·4H_2O$ and 1.5 mL hydrochloric acid (37%)) was prepared in a 50 mL volumetric flask and then transferred to a separatory funnel and was purged for 20 min with nitrogen gas to deoxygenate and prevent oxidation in the solution. An ammonia solution (4.5 M) was prepared and 1 g of prepared Azolla powder was added to it. This solution was transferred to a three-necked flask and heated under nitrogen gas to 80°C. Then, the iron salts were added drop by drop to the ammonia solution under strongly mechanical stirring. Increasing the dropwise of iron mixture leads to a decrease in the diameter and size distribution of MNCs. After the addition of the last drop, the solution was stirred for 10 min under the same conditions. Finally, the black precipitates (MNCs) were collected by a 1.4 Tesla super magnet and washed four times with distilled water, and dried in an oven at 80°C for 4 h.

2.4. Removal of RY 160 dye from aqueous samples using Azolla@Fe_3O_4 MNCs

In order to find the working absorption wavelength, the absorption spectra of RY 160 dye was obtained in the wavelength range of 200–1,100 nm, and based on the spectra, 268 nm was selected as the best wavelength for dye quantitative measurements. All adsorption experiments were performed at room temperature and the amount of adsorbed RY 160 dye was determined from the difference between the initial and final dye concentrations in the solution (Eq. (1)):

$$\% \text{ Removal} = \frac{C_0 - C_t}{C_0} \times 100 \tag{1}$$

where C_0 and C_t are initial and equilibrium concentrations of RY 160 dye after treatment with adsorbent, respectively. In the proposed procedure, to gain maximum adsorption efficiency, various parameters affecting the dye removal efficiency including pH (2, 3, 4, and 5), agitation or contact time (5, 10, 15, and 20 min), sorbent weight (0.05, 0.15, 0.1, and 0.3 g), ionic strength (0, 0.05, 0.1, and 0.25 mol L^{-1}), and volume of sample (25, 50, 75, and 100 mL) were studied and optimized with Taguchi orthogonal array design using L$_{16}$ array (five factors at four levels). The main purpose of the Taguchi design was to determine the optimal conditions. Accordingly, 16 experiments were designed with Minitab 18 software and the experiments were performed in random order to minimize the errors of the method. According to the results of 16 programmed experiments and the ANOVA calculations, the optimal conditions (for solutions containing 50 mg L^{-1} of RY 160 dye) were obtained.

3. Results and discussion

3.1. Characterization of synthesized MNCs

MNCs were studied by SEM to determine the morphology, shape, and size estimation of MNCs (Fig. 2). As shown in Figs. 2a–d, the comparison of SEM images of Azolla before and after magnetization showed the presence of magnetite nanoparticles with particle size less than 40 nm on the surface of Azolla@Fe$_3$O$_4$.

The elemental analysis was also used to confirm the existence of magnetite in the structure of MNCs. The atomic composition of non-magnetic Azolla was evaluated by EDX analysis as C (56.3% wt.), O (36.5% wt.), and other elements including Na, K, Si, Al, Mg, and Ca lower than 9%. The EDX analysis of Azolla@Fe$_3$O$_4$ showed the presence of Fe (26.3%) in the structure that equals to the presence of 0.46 g magnetite per grams of Azolla@Fe$_3$O$_4$.
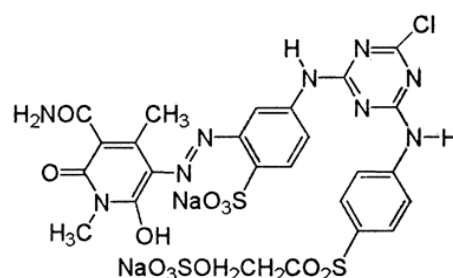
Fig. 1. Chemical structure of RY 160 dye.
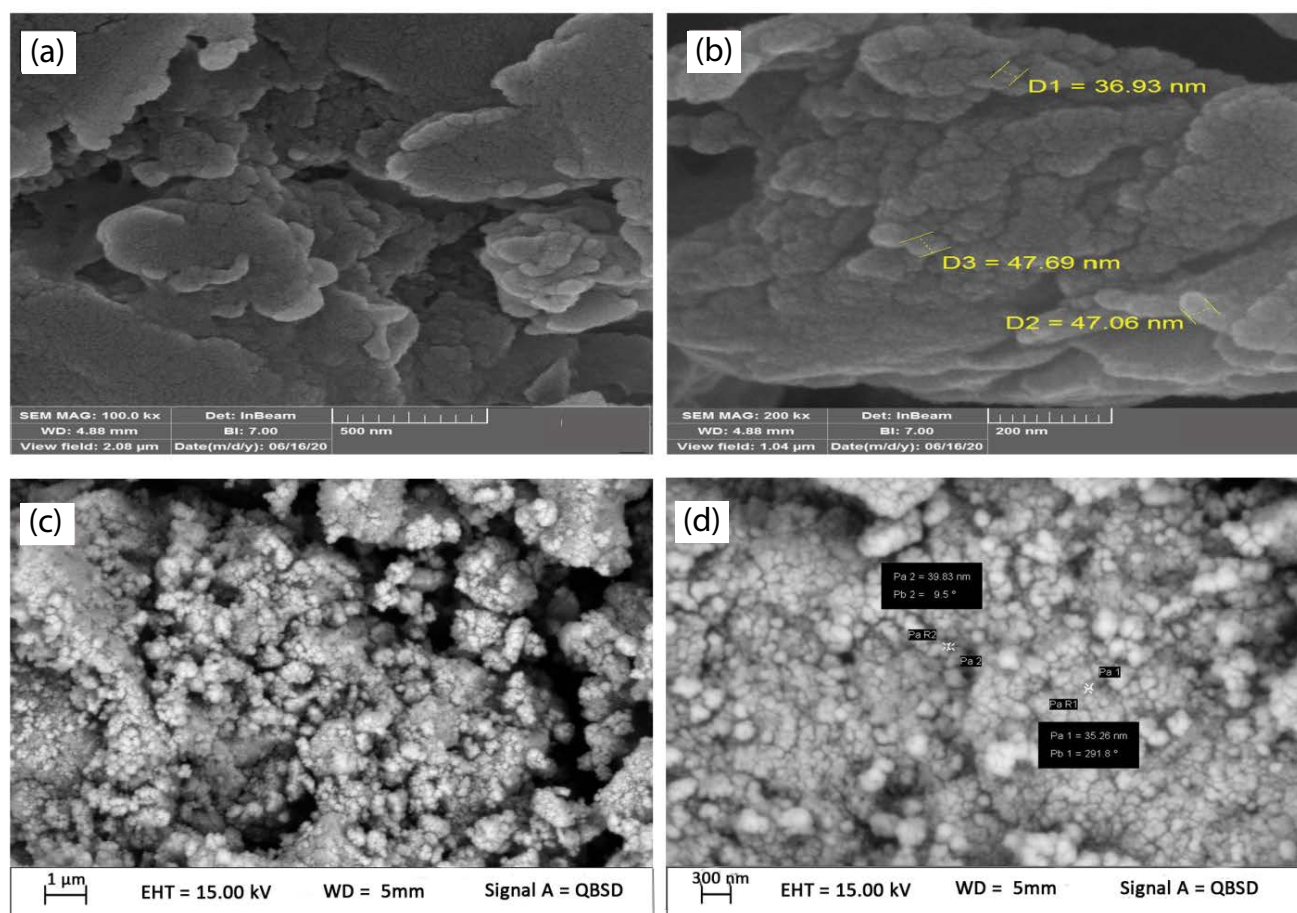
Fig. 2. SEM image of (a and b) Azolla, (c and d) synthesized Azolla@Fe$_3$O$_4$ with (c) 30 and (d) 50 kx magnification.

FT-IR spectra of bare Fe_3O_4, non-magnetic Azolla, and Azolla@Fe_3O_4 are shown in Figs. 3a–c. The absorption bands in the range of 500–600 cm^{-1} is related to Fe–O vibration bands that are observed in all spectra. After examining the FT-IR results for the Azolla@Fe_3O_4 (Fig. 3c), it was found that the strong absorption band at 580 cm^{-1} is related to the Fe–O stretching vibration. The absorption band at 1,020 cm^{-1} corresponds to the C–O vibration. The absorption band observed at 1,404 cm^{-1} is related to bending vibrations of $(CH_2)_n$. The absorption bands at 1,533 and 1,629 cm^{-1} correspond to RCONHR′ and $RCONH_2$, respectively. The absorption bands at 3,409 and 3,425 cm^{-1} are related to the stretching vibrations of the O–H bond. The results confirm the structure of the Azolla@Fe_3O_4.

3.2. Optimization of effective factors on the removal efficiency of RY 160 dye

In this study, the Taguchi orthogonal array design was used to achieve optimum conditions and increase the performance of dye removal by saving time and cost. In all optimization experiments, a constant dye concentration of 50 mg L^{-1} was considered and a magnetic stirrer with a constant stirring rate (400 rpm) was used. The pH of the solutions was adjusted using 0.1 and 0.01 mol L^{-1} HCl and NaOH solutions. After the adsorption period, the solution was placed on a 1.4 Tesla super magnet to separate the MNCs. The supernatant was then removed and the residual concentration of RY 160 dye was determined using a UV-Vis spectrophotometer at 268 nm. The adsorption efficiency of the MNCs was obtained from Eq. (1) (Table 1).

After optimizing experiments according to the Taguchi design, statistical calculations were performed and the mean of the main effects of each factor at different levels was obtained by Minitab software (version 18) (Figs. 4

and 5). Based on the results of experiments and calculations of ANOVA statistical analysis, optimal conditions were obtained as adsorbent weight = 0.15 g, ionic strength = without the addition of salt, pH = 2, sample volume = 25 mL, and contact time = 10 min.

The effect of ionic strength on RY 160 dye removal efficiency was investigated by the addition of different amounts of NaCl to 50 mg L^{-1} RY 160 solutions. The results (Fig. 4a) showed that as the concentration of NaCl increased, the rate of dye removal decreased. Increasing the salt concentration causes a coating form on the MNC surface and prevents
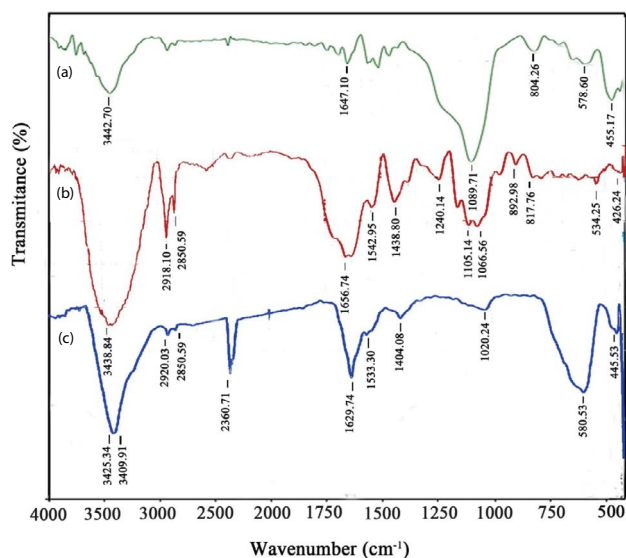
Fig. 3. FT-IR spectra of (a) Fe_3O_4, (b) Azolla, and (c) Azolla@Fe_3O_4 MNC.

Table 1
Taguchi matrix for adsorptive removal of RY 160 dye

Run	Contact time (min)	Sample volume (mL)	Sorbent mass (g)	pH	Ionic strength (mol L^{-1})	Removal (%)
1	5	25	0.05	2	0	88.7
2	5	50	0.1	3	0.05	44.3
3	5	75	0.15	4	0.1	22.0
4	5	100	0.3	5	0.25	23.9
5	10	25	0.1	5	0.25	35.9
6	10	50	0.05	4	0.1	19.0
7	10	75	0.3	2	0.05	88.3
8	10	100	0.15	3	0	65.8
9	15	25	0.15	4	0.05	20.5
10	15	50	0.3	5	0	9.9
11	15	75	0.05	3	0.25	28.0
12	15	100	0.1	2	0.1	61.9
13	20	25	0.3	3	0.1	43.9
14	20	50	0.15	2	0.25	73.8
15	20	75	0.1	4	0	6.3
16	20	100	0.05	5	0.05	14.6
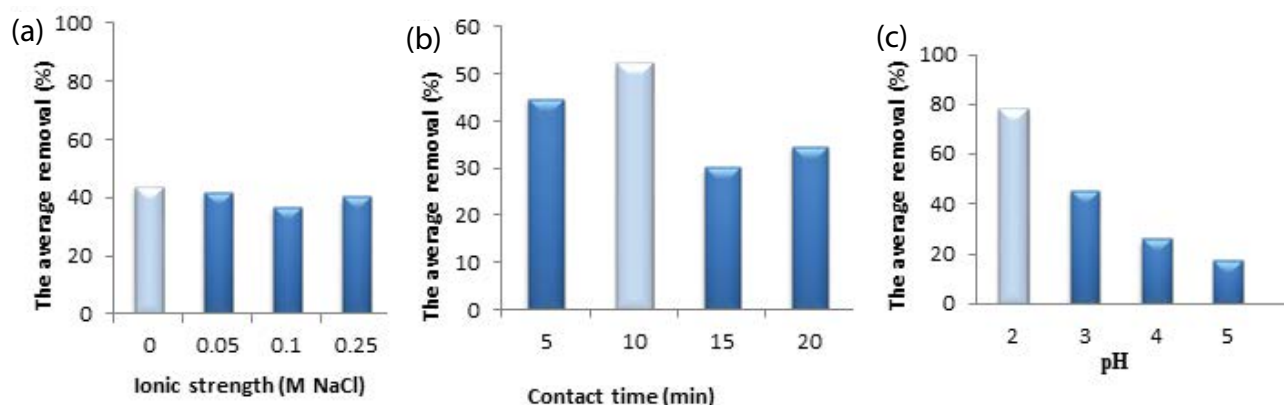
Fig. 4. Curves of an average of the main effects of ionic strength, contact time, and pH at different levels on the removal efficiency of RY 160 dye.

electrostatic interaction between the adsorbent surface and the dye. The results showed the best results are obtained without salt addition. Also, with increasing contact time (Fig. 4b), not only there was no increase in the removal efficiency, but also due to the relative desorption of dye in the solution, there was a slight increase in the absorbance value of the remaining solution, resulting in removal reduction. Therefore, the optimal contact time for removal was 10 min.

Dye adsorption in aquatic solutions depends entirely on the pH of the solution, as pH affects the surface charge of adsorbent and changes the ionization degree of RY 160. Changes in solution pH affect the process of surface adsorption and dissociation of dependent groups at the active surfaces of the adsorbent. As a result, this leads to a change in the kinetics of the adsorption process and the equilibrium properties between the adsorbent and the adsorbate (RY 160 dye). Fig. 4c shows that in acidic pHs, due to the high concentration of H^+ ions in the solution, the active groups at the surface of the MNCs have a partial positive charge and are more prone to the binding of RY 160 anionic dye via electrostatic interactions. A large

reduction in RY 160 dye adsorption efficiency at pHs higher than 2 is explained by the reduction of protonated sites in the surface of Azolla@Fe_3O_4 MNCs. This result is in agreement with our previous study in the removal of RY 160 with magnetite CMK-8 ordered mesoporous carbon [19].

The effect of adsorbent weight on the RY 160 dye removal is shown in Fig. 5a. The adsorbent weight plays a significant role in the adsorption process due to its relationship with the adsorbent capacity. At an adsorbent weight of 0.15 g, a significant amount of RY 160 dye was adsorbed, so the weight of 0.15 g of the adsorbent was selected as the optimal value. No significant change in the removal efficiency was observed with increasing adsorbent weight, despite there was an expectation of an increase in the removal efficiency with an increase in the area of active and effective surface area.

To investigate the effect of sample volume, dye solutions with a concentration of 50 mg L^{-1} were prepared in volumes of 25–100 mL. According to the obtained results (Fig. 5b), in smaller volumes, due to less space for particle motion, the possibility of collision of the dye with the proposed
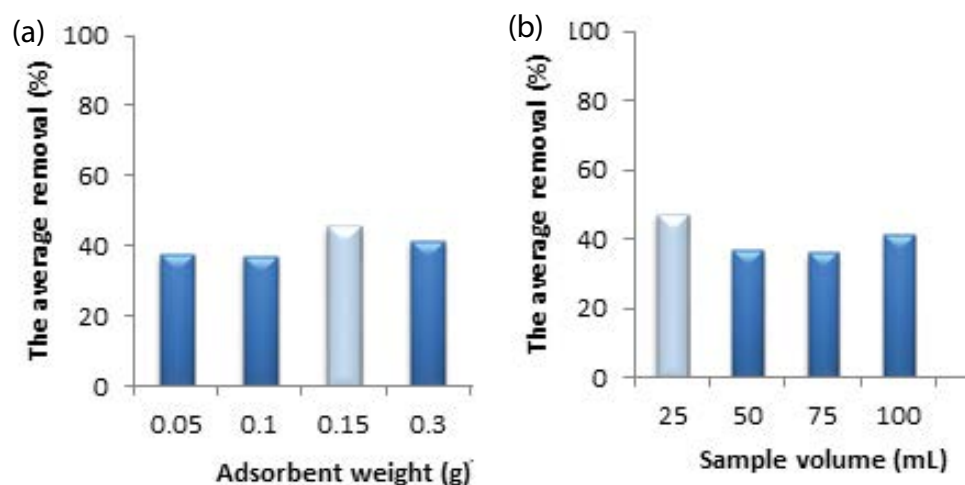
Fig. 5. Curves of an average of the main effects of adsorbent weight (a) and sample volume (b) at different levels on the removal efficiency of RY 160 dye.

adsorbent increases, and the removal efficiency increases. Therefore, the volume of 25 mL was selected as the optimal sample volume for the next steps.

3.3. Confirmation of the optimum conditions

To investigate the reliability of the obtained optimum values, five repetitive adsorption experiments were done on the 50 mg L^{-1} of RY 160 dye solutions at the optimum conditions (sample volume: 25 mL, pH = 2, adsorbent dosage: 0.15 g, contact time: 10 min, and ionic strength: without salt addition). After the adsorption process, the dye residual concentration was determined spectrophotometrically and the removal efficiencies were obtained using Eq. (1). The results exhibited a mean removal efficiency of 97.8% ± 0.5.

3.4. Kinetic studies

Adsorption kinetic models are used to understand the mechanism of the sorption process, such as adsorption, chemical reaction, or penetration mechanism. In order to determine the controlling mechanism of the adsorption process, four kinetic models including pseudo-first-order, pseudo-second-order, Elovich, and intraparticle diffusion models were investigated (Table 2).

Parameters and correlation coefficients of these models were calculated at a constant temperature of 25°C ± 2°C in the time intervals of 30 s, 1, 2, 3, 4, 5, 10, 15, 25, 45, 60, and 90 min at two conditions including (a) 25 mL RY 160 dye sample (50 mg L^{-1}), using 0.15 g MNCs and (b) 100 mL RY 160 dye sample (100 mg L^{-1}) using 0.3 g MNCs. The results are shown in Table 2, where q_e and q_t indicate adsorption capacities at equilibrium and time t (mg g^{-1}), respectively. On the other hand, K_1 (min^{-1}) and K_2 (g mg^{-1} min^{-1}) show the rate constant of pseudo-first-order and second-order adsorption, respectively. In the pseudo-second-order kinetic model, it is assumed that the adsorption process is controlled by chemical sorption.

As shown in Table 2, the correlation coefficient (R^2) of the second-order kinetic model was more than the other models (R^2 = 1, Fig. 6). So, it was chosen as a suitable model.

By this model, when the initial dye concentration rose from 50 to 100 mg L^{-1}, the value of K_2 (g mg^{-1} min^{-1}) for the pseudo-second-order model was reduced from 10.81 to 0.056 g mg^{-1} min^{-1}. Also, $q_{e,\mathrm{cal}}$ (mg g^{-1}) raised from 8.78 to 30.21 mg g^{-1}. This result indicates the applicability of the pseudo-second-order kinetic model to describe the adsorption process. In addition, it shows that chemical reaction occurs during adsorption of RY 160 dye on the surface of Azolla@Fe$_3$O$_4$ MNCs.

3.5. Study of adsorption isotherms

The relationship between the adsorbed chemical and its equilibrium concentration in solution at constant temperature is defined as an isothermal adsorption model that is important in designing an adsorption system. The pattern of the isotherm shows information about the tendency of the surface to be adsorbed and the possible methods of adsorption. The most common way to examine surface isotherms is to determine the concentration of the species in the solution before and after the removal process. To study the adsorption isotherms, the experiments were performed at three times 10, 25, and 50 min using solutions with concentrations of 10, 25, 50, 75, 100, and 250 mg L^{-1} of RY 160 dye. Langmuir (Eq. (2)), Freundlich (Eq. (3)), and Temkin (Eq. (4)) adsorption isotherm models were studied, and based on the results, adsorption follows Freundlich isotherm model (Fig. 7, Table 3). So, the adsorption process is multi-layered.

$$\frac{C_e}{q_e} = \frac{1}{K_L q_m} + \frac{C_e}{q_m} \tag{2}$$

$$\log q_e = \log\left(K_f\right) + \frac{1}{n}\log\left(C_e\right) \tag{3}$$

$$q_e = \frac{RT}{b\ln\left(K_T\right)} + \frac{RT}{b\ln\left(C_e\right)} \tag{4}$$

where C_e, q_e, q_m, and K_L are the equilibrium concentration of RY 160 dye solution (mg L^{-1}), adsorption

Table 2
Equations and the results of kinetic calculations in two RY 160 concentrations of 50 and 100 mg L^{-1}

Kinetics	Equation	Parameters	50 mg L^{-1} RY 160		100 mg L^{-1} RY 160	
			Values	R^2	Values	R^2
Pseudo-first-order	$\log\left(q_e - q_t\right) = \log\left(q_e\right) - \dfrac{K_1}{2.333}t$	K_1 (min^{-1})	−0.2948	0.9369	−2.169	0.8255
		q_e (mg g^{-1})	0.375		0.865	
Pseudo-second-order	$\dfrac{t}{q_t} = \left(\dfrac{1}{k_2 q_e^2}\right) + \left(\dfrac{1}{q_e}\right)$	q_e (mg g^{-1})	30.21	1	8.78	1
		K_2 (g min^{-1} mg^{-1})	0.056		10.81	
Elovich	$q_t = \dfrac{1}{b}\ln\left(ab\right) + \dfrac{1}{b}\ln t$	a (mg g min^{-1})	Curve is non-linear	0.8003	Curve is non-linear	0.4574
		b (g mg^{-1})				
Intraparticle diffusion model	$q_t = k_{\mathrm{dif}}t^{0.5} + C$	C (mg g^{-1})	8.4614	0.1936	20.542	0.5108
		k_{dif}	0.0524		1.3665	
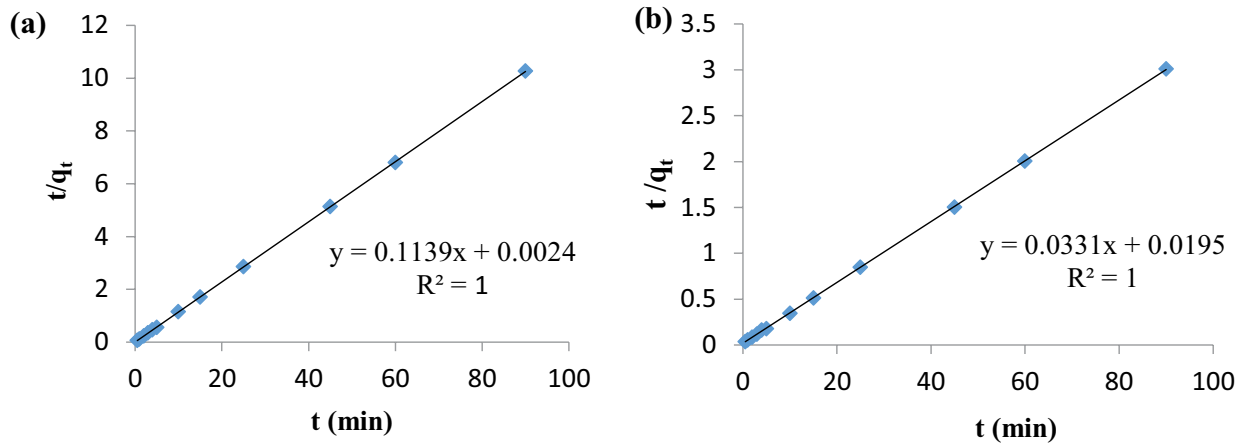
Fig. 6. Pseudo-second-order kinetic model for RY 160 dye removal in concentrations (a) 50 mg L^{-1} (25 mL) and (b) 100 mg L^{-1} (100 mL).
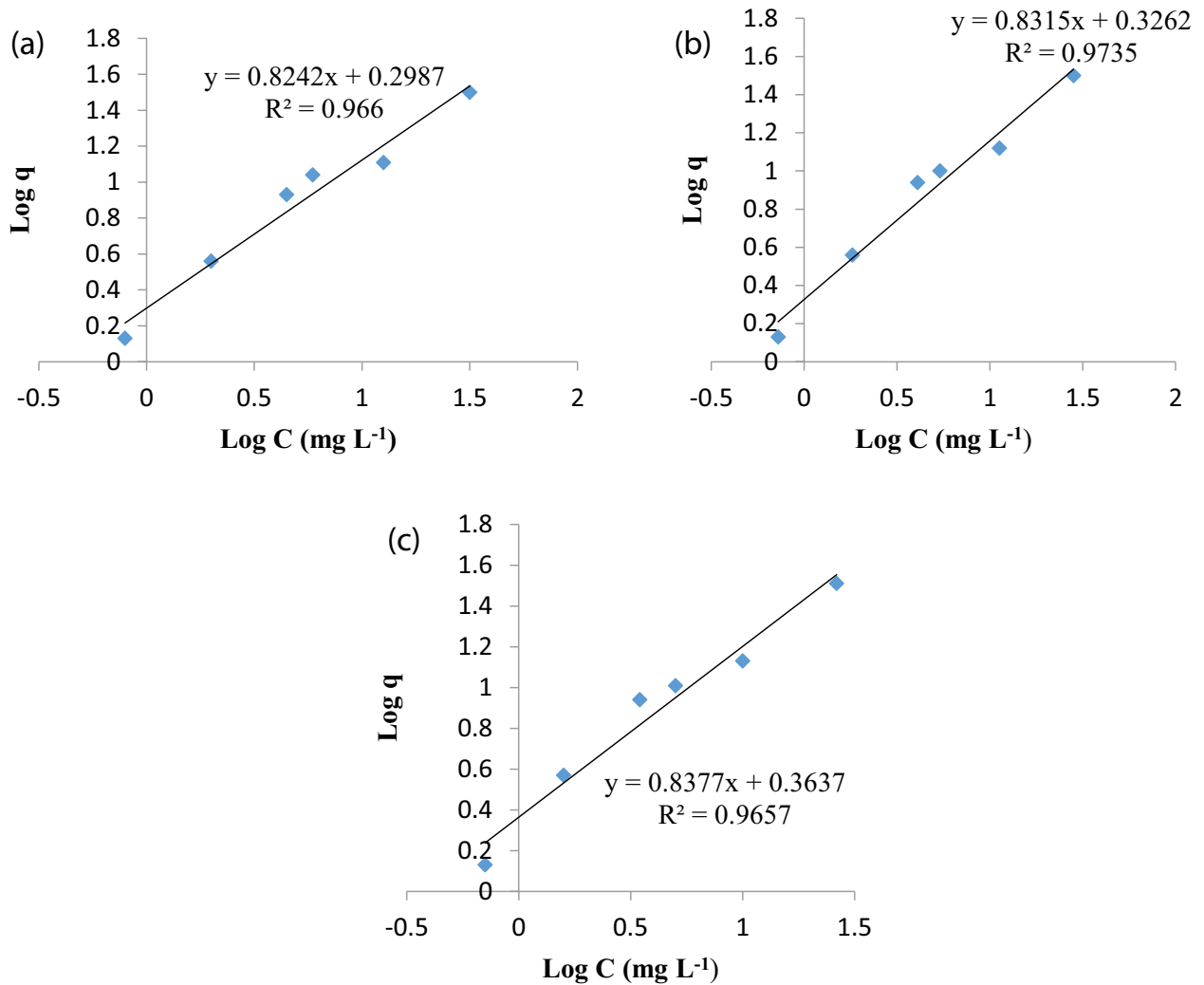
Fig. 7. Freundlich adsorption isotherms, contact time (a) 10 min, (b) 25 min, and (c) 50 min.

Table 3
Results of adsorption isotherm

	Langmuir isotherm			Freundlich isotherm			Temkin isotherm		
	$\dfrac{C_e}{q_e}=\dfrac{1}{Kq_m}+\dfrac{C_e}{q_m}$			$\log q_e=\log\left(K_F\right)+\dfrac{1}{n}\log\left(C_e\right)$			$q_e=\dfrac{RT}{b\ln\left(K_T\right)}+\dfrac{RT}{b\ln\left(C_e\right)}$		
Time (min)	q_m (mg g^{-1})	K_L (L mg^{-1})	R^2	K_F	n	R^2	K_T (L g^{-1})	RT/b	R^2
10	62.89	0.0294	0.6959	1.99	1.21	0.9660	0.783	9.9031	0.8364
25	65.36	0.0310	0.7122	2.12	1.20	0.9735	0.866	9.9539	0.8244
50	63.69	0.0363	0.6997	2.31	1.19	0.9657	0.926	10.242	0.8478

Table 4
Results of removal of 50 mg L^{-1} RY 160 dye from real sample

Real samples	Sample absorbance after spiking dye	Sample absorbance after dye removal	Removal efficiency (%)
Tolamshahr River water	1.34	0.22	83.5 ± 0.8
Sepidrud River water	1.24	0.23	81.4 ± 1.1
Well water	1.10	0.20	81.8 ± 0.8
Tap water	1.08	0.12	90.0 ± 0.4

capacity at the equilibrium time (mg g^{-1}), maximum monolayer adsorption capacity (mg g^{-1}), and equilibrium adsorption constant (L mg^{-1}), respectively. In the Freundlich model, K_F and $1/n$ are Freundlich constant (L g^{-1}) and the intensity of adsorption, respectively. In Temkin isotherm, b (J mol^{-1}) is Temkin constant which is related to the heat of sorption and K_T (L g^{-1}) is Temkin isotherm constant.

According to the isotherm data, the adsorption data obey the Freundlich isotherm model that shows multi-layer adsorption on the heterogeneous surface. In this study, n value of 1.2 at 10, 25, and 50 min shows good adsorption.

3.6. Investigating the adsorption efficiency on real samples

The capability of the synthesized adsorbent to remove RY 160 dye from real samples was investigated with different matrixes including two river waters (Tolamshahr and Sepidrud Rivers), well water, and tap water. These samples were provided from Rasht city (Gilan Province, Iran). For this, firstly, samples were contaminated with 50 mg L^{-1} RY 160 dye and then removal experiments were performed under optimum conditions (pH = 2, without adding salt, sample volume = 25 mL, adsorbent weight = 0.15 g, and contact time = 10 min). The dye concentration before and after the process was determined by UV-Vis spectrophotometer. Results of removal efficiency of RY 160 dye in real samples are summarized in Table 4.

3.7. Reusability of Azolla@Fe₃O₄ MNCs for RY 160 dye removal

Reusability of an adsorbent without a significant decrease in its sorption efficiency is an important factor in adsorption studies. In order to find the reusability of the proposed Azolla@Fe₃O₄ MNCs, several repetitive

experiments were conducted at optimum conditions. After desorption of RY 160 dye with 0.05 M NaOH solution, the recovered MNCs was reused and the observations indicate that after 15 repetitive adsorption process, the removal efficiency was higher than 95%.

3.8. Comparison of the applicability of synthesized Azolla@Fe₃O₄ MNCs with other adsorbents for RY 160 dye removal

The efficiency of synthesized Azolla@Fe₃O₄ MNCs for removal of RY 160 dye was compared with other adsorbents and the results are summarized in Table 5. According to this table, it can be observed that the removal efficiency of synthesized Azolla@Fe₃O₄ is more than magnetite mesoporous carbon [19]. Also, its adsorption was more than other adsorbents for different reactive yellow dyes [24,26,29]. Comparing Azolla@Fe₃O₄ with chitosan@Fe₃O₄ as natural adsorbents showed that the removal efficiency of Azolla@Fe₃O₄ is more than chitosan@Fe₃O₄ [26]. As seen, the synthesized Azolla@Fe₃O₄ has acceptable adsorption capacity and its ability is comparable with other adsorbents.

4. Conclusion

In this research, a nanocomposite of Azolla@Fe₃O₄ was synthesized by a simple method and was applied for the first time for the removal of RY 160 dye. The cost-effectiveness and availability of this nanocomposite are one of its unique properties. The results of this research showed that 0.15 g MNCs can remove RY 160 dye from solution with a removal efficiency of more than 97% in a short time (10 min). Synthesized Azolla@Fe₃O₄ MNCs can be reused 15 times with removal efficiency higher than 95%. The results of adsorption kinetics revealed that the

Table 5
Comparison of kinetics and isothermic models of synthesized Azolla@Fe_3O_4 MNCs with other adsorbents for RY 160 dye removal

Adsorbent	Dye	Kinetic model	Isothermic model	q_{max} (mg g^{-1})	Reference
Magnetite mesoporous carbon	Reactive yellow 160	Pseudo-second-order	Langmuir	62.89	[19]
Magnetite mesoporous carbon@SO_3H	Safranin O	Pseudo-second-order	Freundlich	88.50	[20]
Fe_3O_4@SiO_2@SBA-3-SO_3H	Safranin O	Pseudo-second-order	Freundlich	–	[21]
Fe_3O_4@SiO_2-APTES	Reactive black 5	Pseudo-second-order	Langmuir	56.49	[22]
Magnetic graphene oxide	Reactive black 5	Pseudo-second-order	Langmuir	164	[23]
Fe_3O_4@SiO_2@IL NPs	Reactive yellow 15	Pseudo-second-order	Langmuir	63.69	[24]
CTAB@Fe_3O_4	Reactive red 198	Pseudo-second-order	Langmuir	63.9	[25]
Chitosan@Fe_3O_4	Reactive yellow 145	–	Langmuir	47.62	[26]
IL@Fe_3O_4	Reactive black	–	Langmuir	161.29	[27]
Ionic liquid coated Fe_3O_4 MNPs	Reactive orange 122	Pseudo-second-order	Freundlich	51.54	[28]
1-Octyl-3-methylimidazolium	Reactive red 141	–	Langmuir	71.4	[29]
bromide coated Fe_3O_4	Reactive yellow 81	–	Langmuir	62.5	
Fe_3O_4@SiO_2@TiO_2–NH_2	Acid fuchsin	Pseudo-second-order	Freundlich	188.67	[30]
Coffee@Fe_3O_4 MNCs	Methylene blue	Pseudo-second-order	Langmuir	88.49	[31]
Peanut husk@Fe_3O_4 MNCs				74.62	
Pumice powder	Methylene blue	Pseudo-second-order	Langmuir	>90	[32]
Manganese-coated pumice	Malachite green	Pseudo-second-order	Langmuir	99.9	[33]
Azolla@Fe_3O_4	Reactive yellow 160	Pseudo-second-order	Freundlich	97.8	This research

pseudo-second-order model describes the adsorption of RY 160 dye on this adsorbent. Also, adsorption followed the Freundlich isotherm model and so, the adsorption process is multi-layered. Regarding the high cost of other removal methods, readily separation of Azolla@Fe_3O_4 MNCs from the solution using an external magnet, and also its reusability for several times, making it an economical and effective adsorbent in anionic dyes removal from aquatic solutions.

Acknowledgment

References

[1] S.H. Chen, J. Zhang, C.L. Zhang, Q.Y. Yue, Y. Li, C. Li, Equilibrium and kinetic studies of methyl orange and methyl violet adsorption on activated carbon derived from *Phragmites australis*, Desalination, 252 (2010) 149–156.

[2] F. Çolak, N. Atar, A. Olgun, Biosorption of acidic dyes from aqueous solution by *Paenibacillus macerans*: kinetic, thermodynamic and equilibrium studies, Chem. Eng. J., 150 (2009) 122–130.

[3] N. Kannan, M. Meenakshi Sundaram, Kinetics and mechanism of removal of methylene blue by adsorption on various carbons—a comparative study, Dyes Pigm., 51 (2001) 25–40.

[4] A. Afkhami, R. Moosavi, Adsorptive removal of Congo red, a carcinogenic textile dye, from aqueous solutions by maghemite nanoparticles, J. Hazard. Mater., 174 (2010) 398–403.

[5] L.H. Zhang, P.J. Li, Z.Q. Gong, X.M. Li, Photocatalytic degradation of polycyclic aromatic hydrocarbons on soil surfaces using TiO_2 under UV light, J. Hazard. Mater., 158 (2008) 478–484.

[6] M. Verma, A.E. Ghaly, Treatment of remazol brilliant blue dye effluent by advanced photo oxidation process in TiO_2/UV and H_2O_2/UV reactors, Am. J. Eng. Appl. Sci., 1 (2008) 230–240.

[7] M. Asgher, H.N. Bhatti, Evaluation of thermodynamics and effect of chemical treatments on sorption potential of *Citrus* waste biomass for removal of anionic dyes from aqueous solutions, Ecol. Eng., 38 (2012) 79–85.

[8] J.-H. Chen, Y.-J. Wang, D.-M. Zhou, Y.-X. Cui, S.-Q. Wang, Y.-C. Chen, Adsorption and desorption of Cu(II), Zn(II), Pb(II), and Cd(II) on the soils amended with nanoscale hydroxyapatite, Environ. Prog. Sustainable Energy, 29 (2010) 233–241.

[9] S.R. Kanel, B. Manning, L. Charlet, H. Choi, Removal of arsenic(III) from groundwater by nanoscale zero-valent iron, J. Environ. Sci. Technol., 39 (2005) 1291–1298.

[10] Sh. Shariati, M. Faraji, Y. Yamini, A.A. Rajabi, Fe_3O_4 magnetic nanoparticles modified with sodium dodecyl sulfate for removal of Safranin O dye from aqueous solutions, Desalination, 270 (2011) 160–165.

[11] A. van Amerongen, D. Barug, M. Lauwaars, Eds., Rapid Methods for Biological and Chemical Contaminants in Food and Feed, Wageningen Academic Publishers, Wageningen, 2005.

[12] M. Franzreb, M. Siemann-Herzberg, T.J. Hobley, O.R.T. Thomas, Protein purification using magnetic adsorbent particles, Appl. Microbiol. Biotechnol., 70 (2006) 505–516.

[13] I. Safarik, M. Safarikova, Magnetic techniques for the isolation and purification of proteins and peptides, Biomagn. Res. Technol., 2 (2004) 7, doi: 10.1186/1477-044X-2-7.

[14] U. Jeong, X. Teng, Y. Wang, H. Yang, Y. Xia, Superparamagnetic colloids: controlled synthesis and niche applications, Adv. Mater., 19 (2007) 33–60.

[15] C. van Hove, Azolla and Its Multiple Uses with Emphasis on Africa, Food and Agriculture Organization of the United Nations, Rome, Italy, 1989, p. 53.

[16] K. Giridhar, D. Rajendran, Cultivation and Usage of Azolla as Supplemental Feed for Dairy Cattle, In: Value Addition of Feed and Fodder for Dairy Cattle, NIANP, June 27–July 6, 2013, pp. 32–34.

[17] A. Kumar, Azolla as Cattle Feed, Talanta Institute of Social Sciences, 2011, p. 54.

[18] W. Raja, P. Rathaur, S.A. John, P.W. Ramteke, Azolla: an aquatic pteridophyte with great potential, Int. J. Res. Biol. Sci., 2 (2012) 68–72.

[19] S. Toutounchi, Sh. Shariati, K. Mahanpoor, Synthesis of nano-sized magnetite mesoporous carbon for removal of reactive yellow dye from aqueous solutions, Appl. Organomet. Chem., 33 (2019) e5046.

[20] S. Toutounchi, Sh. Shariati, K. Mahanpoor, Sulfonic acid functionalized magnetite nanomesoporous carbons for removal of Safranin O from aqueous solutions, Desal. Water Treat., 53 (2019) 253–263.

[21] S.M. Seyed Danesh, H. Faghihian, Sh. Shariati, Sulfonic acid functionalized SBA-3 silica mesoporous magnetite nanocomposite for Safranin O dye removal, Silicon, 11 (2019) 1817–1827.

[22] Z. Bozorgpanah Kharat, M. Mohammadi Galangash, A. Ghavidast, M. Shirzad-Siboni, Removal of reactive black 5 dye from aqueous solutions by $Fe_3O_4@SiO_2$-APTES nanoparticles, Caspian J. Environ. Sci., 16 (2018) 287–301.

[23] G.Z. Kyzas, N.A. Travlou, O. Kalogirou, E.A. Deliyanni, Magnetic graphene oxide: effect of preparation route on reactive black 5 adsorption, Materials, 6 (2013) 1360–1376.

[24] F. Golmohammadi, M. Hazrati, M. Safari, Removal of reactive yellow 15 from water sample using a magnetite nanoparticles coated with covalently immobilized dimethyl octadecyl [3-(trimethoxysilylpropyl)]ammonium chloride ionic liquid, Microchem. J., 144 (2019) 64–72.

[25] M. Faraji, Y. Yamini, M. Rezaee, Magnetic nanoparticles: synthesis, stabilization, functionalization, characterization, and applications, J. Iran. Chem. Soc., 7 (2010) 1–37.

[26] N.A. Kalkan, S. Aksoy, E.A. Aksoy, N. Hasirci, Adsorption of reactive yellow 145 onto chitosan coated magnetite nanoparticles, J. Appl. Polym. Sci., 124 (2012) 576–584.

[27] T. Poursaberi, M. Hassanisadi, Magnetic removal of reactive black 5 from wastewater using ionic liquid grafted-magnetic nanoparticles, Clean: Soil Air Water, 41 (2013) 1208–1215.

[28] S.H. Ahmadi, P. Davar, A. Manbohi, Adsorptive removal of Reactive Orange 122 from aqueous solutions by ionic liquid coated Fe_3O_4 magnetic nanoparticles as an efficient adsorbent, Iran. J. Chem. Chem. Eng., 35 (2016) 63–73.

[29] S. Kamran, H. Tavallali, A. Azad, Fast removal of Reactive Red 141 and reactive yellow 81 from aqueous solution by Fe_3O_4 magnetic nanoparticles modified with ionic liquid 1-octyl-3-methylimidazolium bromide, Iran. J. Anal. Chem., 1 (2014) 78–86.

[30] S. Rahnama, Sh. Shariati, F. Divsar, Synthesis of functionalized magnetite titanium dioxide nanocomposite for removal of Acid fuchsin dye, Comb. Chem. High Throughput Screening, 21 (2018) 583–593.

[31] N. Besharati, N. Alizadeh, Sh. Shariati, Removal of cationic dye methylene blue (MB) from aqueous solution by coffee and peanut husk modified with magnetite iron oxide nanoparticles, J. Mex. Chem. Soc., 62 (2018) 110–124.

[32] K. Sharafi, A.M. Mansouri, A.A. Zinatizadeh, M. Pirsaheb, Adsorptive removal of methylene blue from aqueous solutions by pumice powder: process modelling and kinetic evaluation, Environ. Eng. Manage. J., 14 (2015) 1067–1078.

[33] A. Karami, K. Karimyan, R. Davoodi, M. Karimaei, K. Sharafie, S. Rahimi, T. Khosravi, M. Miri, H. Sharafi, A. Azari, Application of response surface methodology for statistical analysis, modeling, and optimization of malachite green removal from aqueous solutions by manganese-modified pumice adsorbent, Desal. Water Treat., 89 (2017) 150–161.